Indian Journal of Engineering & Materials Sciences
Vol. 29, April 2022, pp. 218-227

# Hot corrosion performance of bare and coated T91 steel under actual and simulated bio-fuel fired boiler environment

Manoj Kumar[a], Deepa Mudgal[a], & Lalit Ahuja[b*]

[a]Department of Mechanical Engineering, Thapar Institute of Engineering and Technology, Patiala, Punjab 1470 01, India

[b]Department of Mechanical Engineering, Sant Longowal Institute of Engineering and Technology, Punjab 148 001, India

*Received: 6 February, 2021; Accepted: 1 September, 2021*

The conventional fuel has now been replaced by bio-fuels, due to an increasing demand of power supply which has only been met through the non-renewable resources so far. However, burning of bio-fuel creates corrosive atmosphere which is different from that of coal and oil firing. Therefore, in the present investigation, bare and coated boiler steel T91 substrates were exposed to real andsimulated bio-fuel fired boiler environment working at high temperature. It was noticed that dense and protective oxide was present on $Cr_3C_2$-NiCr coated T91 steel after 50hours of exposure in the simulated environment which depicts the protective behaviour of the coating and compatibility of coating with steel despite of variation in the composition. However, oxide so formed in actual bio-fuel fired boiler was porous. WC-Co coated T91 steel has undergone severe corrosion by showing the oxide spallation and delamination of the coating from the substrate under a simulated environment. Similar observations were noticed in the actual boiler working at the temperature of 750±50°C.

**Keywords:** Boiler steel, Hot corrosion, Detonation gun, Coating

## 1 Introduction

Accelerated oxidation which occurs because of the presence of fused salt deposits like; $K_2SO_4$, $Na_2SO_4$, NaCl, KCl etc., at elevated temperature can be named as hot corrosion[1]. Nowadays, various auxiliary fuels are being burned in the boilers to save non-renewable fuels. Specific attention has been given to the burning of bio-fuels, such as straw and wood chips, across the globe for power production because of its availability[2]. Burning of different fuels in the boiler creates a more corrosive environment due to the formation of salts species that get deposited on the components, thus accelerating hot corrosion. Nielsen *et al.*[3] investigated the problem of corrosion encountered during the burning of biomass fuel in power plants. They opined that the primary cause of the destruction of the metal component is the presence of chlorine, which is released during the burning of coal and biofuel individually or together in boilers. Chlorine specifically reacts with the protective oxide and converts it into volatile metal chloride. These volatile compounds evaporate through the oxide scale, making protective oxide porous. This phenomenon is known as active oxidation. The porous oxide supports the migration of a corrosive environment towards the substrate oxide interface. Active oxidation is one of the mechanisms through which corrosion accelerates in a boiler environment[4-6]. However, many other corrosive species are present in the boiler and can cause severe damage, such as compounds of calcium and sulfur. It has also been noticed from the literature that the life of the alloys depends upon the working environment. An alloy does not need to behave the samein a gas turbine and a boiler environment. The difference in behaviours is due to the variation in the fuel used for burning. Hence it is necessary to analyze the mechanism of surface degradation of various steels, alloys, and coatings in different aggressive environments. After knowing the mechanism, the best possible alternative can be used in a particular atmosphere.

T91 steel is generally used for the construction of the boiler components. Chatha *et al.*[7], described that, steel T91 on exposure under a molten salt environment at 750°C, it shows intense spalling and sputtering, along with the cracking of edges. Uusitalo *et al.*[8] conducted experiments on high velocity oxy fuel coated specimens, laser-melted HVOF coatings, bare ferritic and austenitic boiler steel under simulated bio-fuel environment. They reported that ferritic steels showed considerably higher weight gain as compared to austenitic steel, which shows less resistance to

*Corresponding author (E-mail: lalit.ahuja003@gmail.com)

corrosion. It is because of the presence of chlorine, active oxidation occurs even at low temperatures. Active oxidation significantly degrades the components of boilers. However, coatings substantially increase the life of steels under the corrosive atmosphere. Thermal spray coatings deposited on steel exhibits excellent resistance to corrosion as compared to bare steels. It is necessary to identify the correct combination of substrate and coating, along with the method of deposition for any environment. The respective coating can delaminate from the substrate despite using the best thermal spray processdue to thermal fluctuation. Also, not all coatings can sustain in all corrosive environments. Among the thermal spray processes, Detonation gun process is known for developing low porosity coating along with very high bond strength[9-12]. Hence, the present work analyses the corrosion behavior of coated and uncoated T91 ferritic steel in real and simulated biofuel fired boiler environment. Ferritic steel has been chosen because of the considerable difference in cost of ferritic and austenitic steel, and this steel is widely used in the boiler. The specimens were coated with two different carbide coatings using Detonation gun technique. Carbides coatings were chosen because of their properties such as good corrosion resistance at high temperature due to presence of chromium and hardness owing to presence of carbide. Carbide based metallic coatings are hard as compared to nickel-based coatings. Apart from corrosion resistance, hardness is also required as the particles formed in the boiler can erode the components. As thermal conductivity is a major concern in the boilers, hence ceramic coatings have not been used. Existing literature related to the $Cr_3C_2$-NiCr indicates that this coating shows good resistance to corrosion in high-temperature aggressive environments[7,11,13-15]. Most of the reported literature discusses the corrosion performance of HVOF coated T91 steel under coal-fired boiler or turbine environment[7,13-15]. However, the performance of detonation gun sprayed $Cr_3C_2$-NiCr coated T91 steel under the actual and simulated biofuel fired boiler has not been investigated so far. Hence, the present study focused on the evaluation of bare and detonation gun coated steel which was hung in the boiler where rice husk and wood has been used as fuel. The experiments were also conducted in laboratory by creating simulated environment.The salt species chosen to create environment was selected from one of the study reported by Uusitalo *et al*[8]. They reported that the environment was present in bio-fuel fired boiler and incinerator environment.

## 2 Materials and Methods

### 2.1 Substrate

Ferritic steel T91 has been chosen for the study which was procured from Cheema Boilers, Punjab. This steel is used for the construction of boiler parts such as heat exchangers and super-heater tubes. After procuring the steel, spark spectroscopy was conducted to know the exact composition of the substrate. The composition of the steel was found to be Fe:balance, C:0.05-.015, Mn:0.3-0.4, P:0.025,S:0.025, Mo:0.87-1.13, Cr:7.5-8.2, Si:0.50. The substrates used for the experiments were cut from a steel plate to a dimension of 20x15x5mm. Prior to experimentation and coating deposition, all the substrates were polished by 220, 400, and 600 grit size emery papers. Alumina polish was also done with 0.3µm size alumina particles suspension.

### 2.2 Coating deposition

Commercially available $Cr_3C_2$-20(NiCr) and WC-12Co coating powders (Praxair) were deposited using detonation gun thermal spray technique available at SVX powder M Surface, Greater Noida, India. Both the coating powders were spherical in shape with size varying from 5µm to 45µm. Figure 1 (a and b) show the SEM along with EDS analysis of both the coating powders. The substrates were grit blasted using alumina grains before coating deposition to increase the adherence of coating on the substrate. Prior to grit blasting, the samples were dipped in acetone and then dried to get rid of contamination on the surface. The parameters of detonation-gun used while coating deposition here as: Firing rate:1-10Hz, water consumption rate: 15-25 lit/min, sound pressure level: 150db. Oxygen, nitrogen, acetylene and air were as working gases with a working pressure of 0.2, 0.4, 0.14 and 0.4 (MPa) respectively. Consumption of gases per shot was $27x10^{-5}m^3$ for oxygen, $5x10^{-5}m^3$ for nitrogen, $23x10^{-5}m^3$ for acetylene and $5x10^{-5}m^3$ for air.

### 2.3 Hot corrosion experiment

The corrosion test at elevated temperature was conducted in a laboratory in a tubular furnace. Cyclic studies were conducted to create a catastrophic atmosphere. The temperature of the furnace was kept at 800°C throughout the 50 cycles. The samples were kept in the tubular furnace using alumina boats for 1 hour individually (one sample in one boat) and then brought to the atmospheric temperature to give thermal fluctuations. After keeping it for 20 minutes in ambient temperature, the weight of specimens with

respective boats was measured by digital weighing balance with accuracy level of 0.1 mg. The cycles were repeated for 50 hours, and the weight change was recorded to establish corrosion kinetics. Before starting experiments, all coated and bare samples were coated with a salt mixture ($40Na_2SO_4$ +$40K_2SO_4$+10NaCl+ 10KCl) to simulate the boiler environment. The salt mixture was made in distilled water. Before the salt coating, the samples were heated in the oven kept at 150°C for 60minutes. Nearly 3-5mg/cm$^2$ salt was coated using a paintbrush. Salt coated samples were again kept in the oven at 150°C to remove moisture content. The heating was done just before starting hot corrosion experiments for almost 1hour. After carrying out experiments in the laboratory, the samples were also hanged in the boiler where 90% rice husk, wood and saw dusk (remaining 10%) was used as fuel.Due to rice husk, the environment in the actual boiler consists of compounds of silicon and calcium in major amount along with compounds of sodium, potassium, sulphur and chlorine. The temperature of the boiler was 750°C. The samples were kept for 48hours near the soot blower. Kanthal wire (grade A) was used to hang the drilled samples. After experiments, the characterization of the corroded substrates was done using SEM/EDS, X-ray mapping and XRD. SEM /EDS analysis was performed to know the surface morphology and elements present in the oxide scale. X-ray mapping was done for the cross-sectional area to know the depth of corrosive attack. XRD was done to identify the phases formed on the corroded substrate.

## 3 Results and Discussion

### 3.1 Visual Analysis

Visual macro-photos were taken after each cycle of hot corrosion. Figure 2 shows the macro-photos of

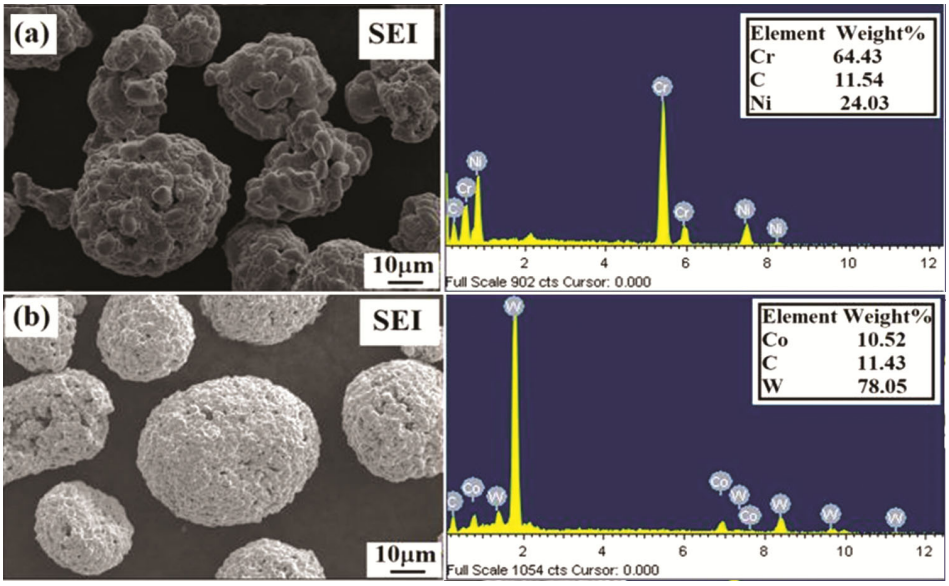


Fig. 1 — SEM/EDS analysis of (a) $Cr_3C_2$-NiCr, and (b) WC-12 Co coating powders.

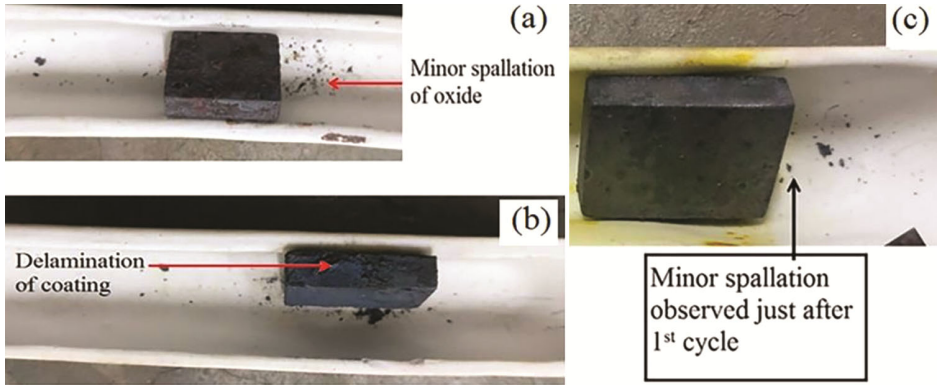


Fig. 2 — Macrophotos showing the condition of (a) bare T91 steel, (b) WC-Co coated steel, and (c) $Cr_3C_2$-NiCr coated T91 steel after exposed in simulated bio-fuel fired boiler environment at 800 °C after 1$^{st}$ cycle.

bare, WC-Co coated T91 and $Cr_3C_2$-NiCr coated T91 steel after hot corrosion run in the laboratoryjust after 1st cycle respectively. It was observed that fragile oxide was formed just after the 1st cycle in case of T91 steel. The fragile nature of the oxide is indicated in the form of spallation present in the boat (Fig. 2(a)). The color of oxide was dark grey, along with reddish-brown patches on the surface. After the 2nd cycle till the 14th cycle, the corrosion was intensified, thereby leading to more spallation. After the 15th cycle, no significant changes were observed. In WC-Co coated T91 steel (Fig. 2(b)), it was seen that the coating had undergone major spallation and initiation of delamination just after the 1st cycle. Cracks also appeared on the surface of the coating. After that, the coating starts delaminating from the steel substrate from all the sides. $Cr_3C_2$-NiCr coated T91 steel (Fig. 2(c)) undergone minor spallation just after 1st cycle. The formation of greenish oxide with dark grey background was also indicated. No, substantially changes were recorded after the 2nd cycle. Figure 3 shows the condition of bare and coated substrates after exposing an actual boiler environment for 48h. Bare T91 (Fig. 3(a)) shows the formation of reddish oxide along with a dark grey background. $Cr_3C_2$-NiCr coated steel (Fig. 3(b)) shows the formation of the dense green color oxide. Whereas, WC-12Co coated T91 steel (Fig. 3(c)) shows the initiation of delamination of coating from the corners.

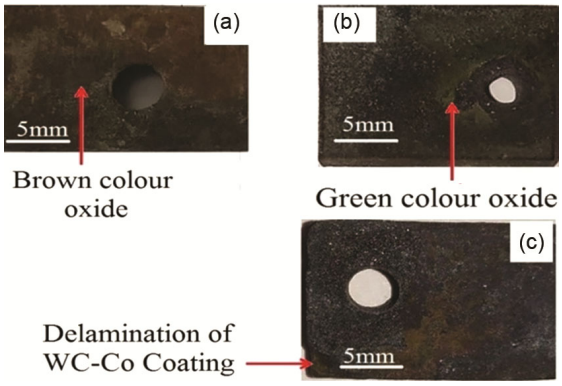


Fig. 3 — Macrophotos of corroded (a) bare, (b) $Cr_3C_2$-NiCr, and (c) WC-Co coated T91 steel on exposure in real boiler environment for 48 hours at 750±50 ºC.

### 3.2 Weight change measurements

A weight gain graph was plotted, showing the weight change/surface area versus number of cycles in Fig. 4(a). It can be clearly seen from the graph that WC-Co coated T91 steel showed very high weight gain starting from the 1st cycle till the 30th cycle. However, after the 31st cycle, the weight gain becomes parabolic. Bare and $Cr_3C_2$-NiCr coated T91 steel both showed minor weight gain in initial cycles after that the weight gain becomes constant. Out of all the three specimens, $Cr_3C_2$-NiCr coated T91 steel showed least weight gain followed by bare T91 steel and WC-Co coated steel respectively. It is well established thatoxidation/corrosion kinetics can be illustrated by a parabolic rate law:

$$Kp = \frac{x^2}{t} \quad \ldots (1)$$

where, $K_p$ = parabolic rate constant, $x$ = the oxide thickness, $t$= time[16]

The $K_p$ for different substrates can be compared whichfurther allows the quantification of the corrosion rate. A higher protective behaviour of oxide can be judged by a small value of $K_p$. A high $K_p$corresponds to a higher rate of reactions thus leads to non-protective conditions. Hence $K_p$ value for all the specimens has been calculated using graphs shown in Fig. 4(b). The graph is plotted for the weight

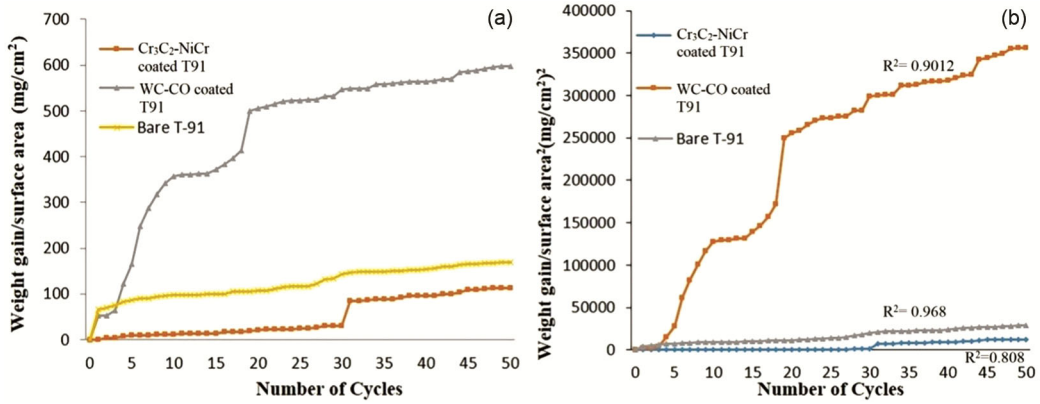


Fig. 4 — (a) (Weight gain/Surface area) (mg/cm$^2$) Versus Number of cycles, and (b) (Weight gain/Surface area) (mg/cm$^2$)$^2$ Versus Number of cycles for bare and coated T91 steel after corrosion under simulated bio-fuel fired boiler atmosphere at 800 °C for 50 cycles.

gain/surface area square ($mg^2/cm^4$) versus time (number of cycles) to establish the rate law for oxidation. The parabolic rate constant can be calculated from the slope of the linear regression fitted line from this graph. The values of the graph clearly depicts that $Cr_3C_2$-NiCr coated T91 ($K_p$= $8.07*10^{-8}g^2cm^{-4}s^{-1}$) shows least $K_p$ value followed by bare T91 steel ($K_p$= $15.35*10^{-8}g^2cm^{-4}s^{-1}$)and the maximum for WC-Co coated T91 steel ($K_p$= $204.1*10^{-8}g^2cm^{-4}s^{-1}$). In the graph, the values of $R^2$ were also shown, which shows the goodness of the linear fit for trend line to the data. It ranges within 0 to 1. Bare T91 has $R^2$ = 0.968 (Fig. 4(b)) which shows that it follows 96.8% linear rate law and 3.2% parabolic rate law. Similarly, $Cr_3C_2$-NiCr coated T91 steel shows 80.8% linear rate law and 19.2% parabolic rate law.

### 3.3 Corrosion rate (MPY)

Weight loss measurement was done for the samples exposed to the actual boiler environment. $Cr_3C_2$ – NiCr coated steel experienced less weight loss, which was about 20 mg. Weight loss in the case of WC-Co steel was high,which is 43 mg, and in case of bare T91 steel thickness loss was found to be 32 mg. The measurement of weight loss was done using Digital weighing balance. Three readings were taken for all the three samples before and after exposing substrates in the boiler. The value of weight loss was further applied to measure the corrosion rate in mils per year (mpy). The corrosion rate was very high for WC-Co coated steel (40.32 mpy) followed by T91 steel (30.94 mpy) and least for $Cr_3C_2$-NiCr coated steel (18.81 mpy)

#### 3.4 SEM/EDS analysis

SEM micrographsof bare, WC-Co and $Cr_3C_2$-NiCr coated T91 steel after corrosion test conducted under actual and simulated boiler environment has been shown in Figs (5-7) with EDS spectrum. It can be inferredfrom the results, that irregular and porous oxide was formed on the surface of bare T91 steel (Fig. 5), having iron and oxygen as major components in both environments. However, Mo was also detected in the simulated environment (Fig. 5(a)). Under the actual boiler test, extra peaks of sulfur, potassium and silicon were also observed. Fine needle-type dense oxide can be observed in case of $Cr_3C_2$-NiCr coated T91steel (Fig. 6 (a)). The EDS analysis indicates that the surface of the specimen mainly has oxygen and chromium. A minor quantity of sodium, potassium and molybdenum were also seen. Molybdenum might have diffused from the substrate. The surface oxide formed on $Cr_3C_2$-NiCr coated steel (Fig. 6(b)) after exposure in the real boiler atmosphere seems to be porous, although the structure remains the same. Major quantity of silicon was recorded on all the samples exposed in the actual boiler. Three different structures of oxides can be clearly seen in WC-Co coated T91 steel in the insert image of Fig. 7(a). EDS analysis shows the presence of oxygen, cobalt and tungsten where clusters oxide was present, whereas, at other sites, iron was also detected. Figure 7(b) clearly indicates two different regions present due to the delamination of the coating during exposure in the actual boiler environment. In Fig. 7(c and d), clusters oxide structure is visible consisting of iron, oxygen, cobalt and tungsten.

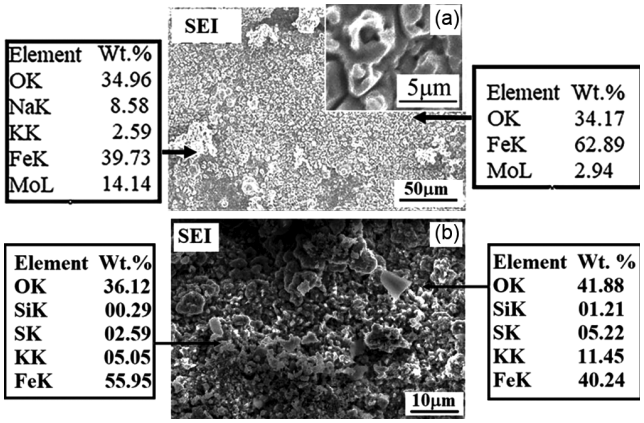


Fig. 5 — SEM images with EDS at some selected sites of bare T91 after subjected to hot corrosion under (a) simulated, and (b) real boiler environment.

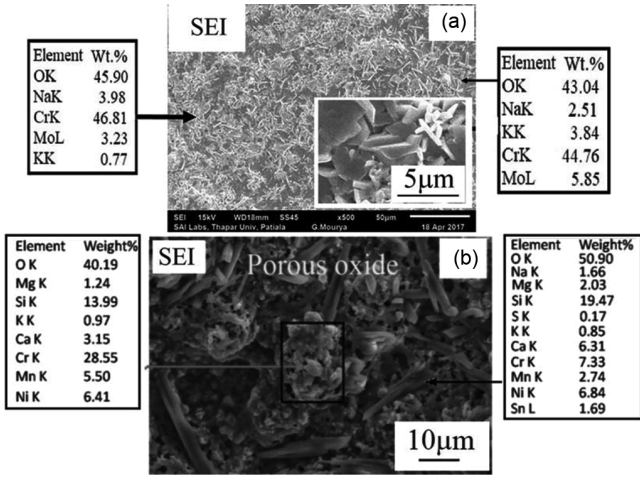


Fig. 6 – SEM images with EDS at some selected sites of $Cr_3C_2$-NiCr coated T91 steel subjected to cyclic hot corrosion under (a) simulated, and (b) real boiler environment.

### 3.4 XRD analysis

XRD graph has been plotted between Intensity and diffraction angle 2θ. The graphs were shown to identify the phases present in the scale formed. The graph of the scale formed on the corroded specimens was shown in Figs 8 and 9. In case of bare T91 steel sample, the formation of oxides such as $Cr_2O_3$, $K_2CrO_4$, $Na_2SO_4$, $K_2MoO_4$, $Fe_2O_3$ and FeS can be seen after exposure in a laboratory furnace. Whereas in boiler environment, peaks of $FeSiO_4$, $Cr_2S_3$ and FeS were found. The major phases identified in the case of $Cr_3C_2$-NiCr coated T91 steel after corrosion test in laboratory furnace were $Cr_2O_3$, $CrCl_3$, $K_2CrO_4$, $Na_2SO_4$ and $Cr_3S_4$. In the boiler environment, peaks of $NiCr_2O_4$, $K_2CrO_4$, $Mg_2SiO_4$ and $Ni_2SiO_4$ were detected. In the case of WC-Co coated steel, the major oxides formed after exposure in a simulated environment were $Cr_2O_3$, $CrCl_3$, $Na_2SO_4$, $KClO_3$ and $Co_3O_4$. In an actual boiler environment, peaks of $CoCr_2O_4$, $CoWO_4$ and $FeWO_4$ were seen.

### 3.5 Elemental X-ray Mapping

Figures (10-15) represents the X-ray mapping of cross-sectional area for corroded bare, WC-Co and $Cr_3C_2$-NiCr coated T91 steel after subjected to corrosion under simulated and in real boiler environment. The elements present in the oxide layer that was found by X-ray mapping were C, O, Cr, Fe,

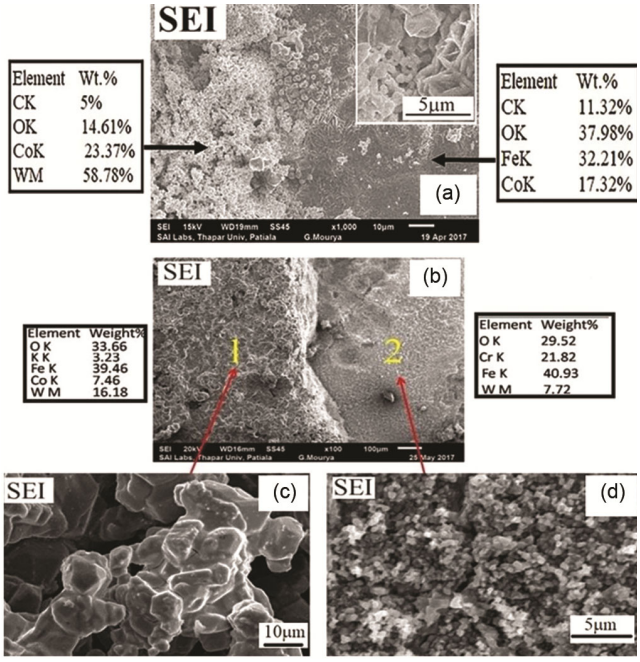


Fig. 7 — SEM image with EDS at selected location of WC-Co coated T91 steel subjected to cyclic hot corrosion under (a) simulated, and (b-d) actual-fuel fired environment

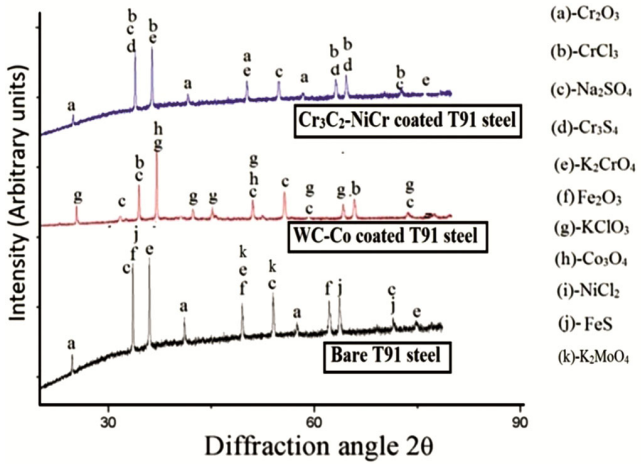


Fig. 8 — XRD graph of bare, $Cr_3C_2$-NiCr, and WC-Co coated T91 steel after hot corrosion under simulated bio-fuel fired boiler environment at 800 °C for 50 cycles.

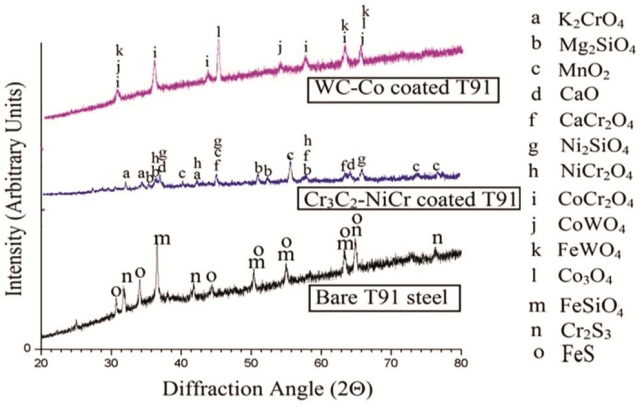


Fig. 9 — XRD graph of bare, $Cr_3C_2$-NiCr, and WC-Co coated T91 steel after hot corrosion under actual bio-fuel fired boiler environment at 750±50 ºC for 48 hours.

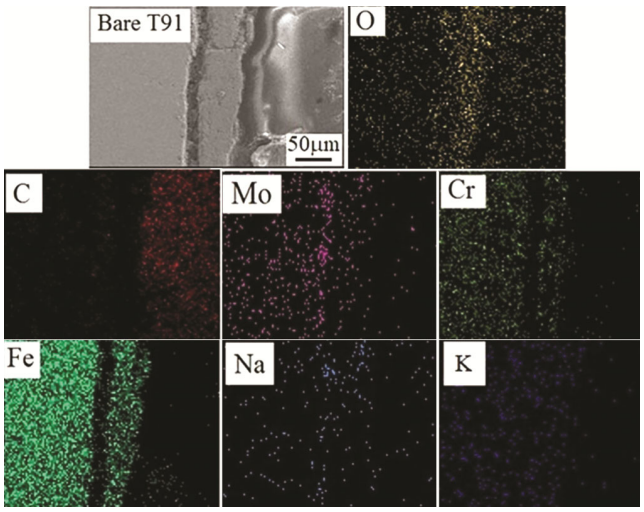


Fig. 10 — X-Ray mapping of bare T91 steel after exposure in molten salt environment at 800°C for 50 cycles in tubular furnace.

Na and Mo in case of a bare T91 sample after exposure in a simulated environment (Fig.10). It was noticed that under both the environment, bare T91 steel showed the presence of oxygen, chromium, and iron (Figs 10 and 11). Chromium was mainly present at the interface of oxide and substrate, whereas iron was seen throughout the oxide layer. The cross-sectional analysis also indicates that the $Cr_3C_2$-NiCr coating remains intact to the T91 substrate (Figs 12 and 13), and the elements present in the oxide were C, O, Fe, Ni and Cr. Presence of oxygen can be seen throughout the coating. In WC-Co coated T91 steel (Figs 14 and 15), the coating got delaminated from the substrate. A thin layer of tungsten can be seen on the top of oxide layer along with chromium and iron. The observations werethe same for both the specimens exposed in simulated as well as the actual environment.

**3.6 Discussion**

The visual analysis clearly shows that $Cr_3C_2$-NiCr coated T91 steel suffered from minor spallation in the simulated (Fig. 2(c)) and actual (Fig. 3(b)) biofuel fired boiler environment. However, bare T91 steel (Figs (2(a) and 3(a))) shows the formation of fragile oxide mainly red in color. The presence of reddish oxide on the surface of T91 depicts the formation of iron oxide just after the 1st cycle. In the later cycle, it was also observed that the oxide of the color changes to a dark grey background, which depicts the formation of chromium oxide. Therefore, it can be predicted that un-protective oxides of iron and chromium might have formed during the thermal cycles enhancing the corrosion in the metal. Macro photos of WC-Co coated T91 steel after exposure in laboratory furnace (Fig. 2(b)) and in actual environment (Fig. 3(c)) clearly shows that the coating got delaminated from the substrate. This might have

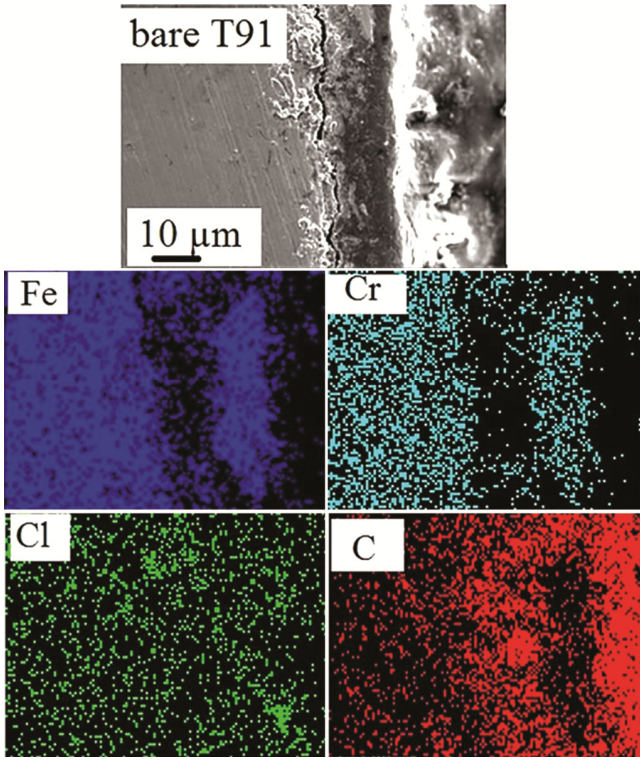


Fig. 11 — X-Ray mapping of bare T91 steel after exposure in real bio-fuel fired boiler environment at 750±50 ºC for 48 hours.

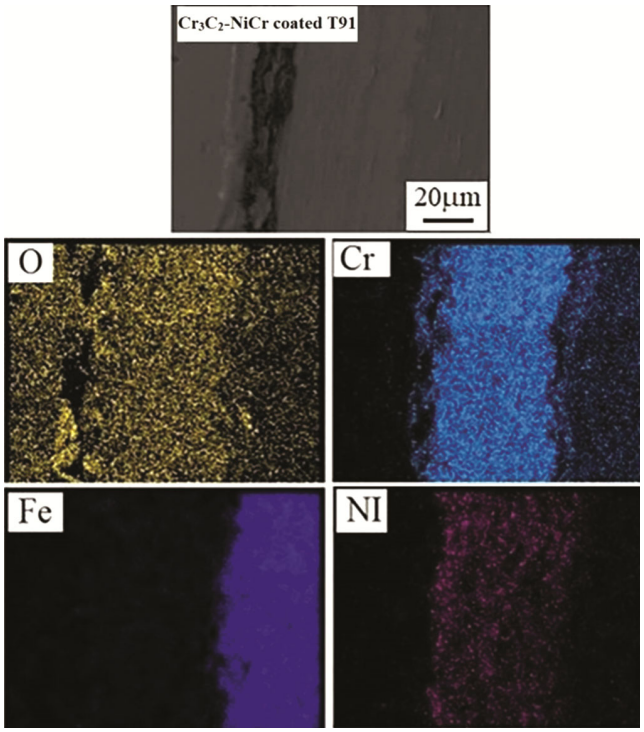


Fig. 12 — X-Ray mapping of $Cr_3C_2$-NiCr coated T91 after exposure in molten salt environment at 800 °C for 50 cycles in tubular furnace.

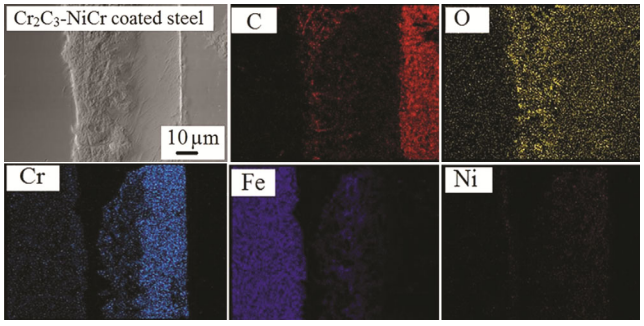


Fig. 13 — X-Ray mapping of $Cr_3C_2$-NiCr coated T91 steel after exposure in real bio-fuel fired boiler environment at 750±50 ºC for 48 hours.

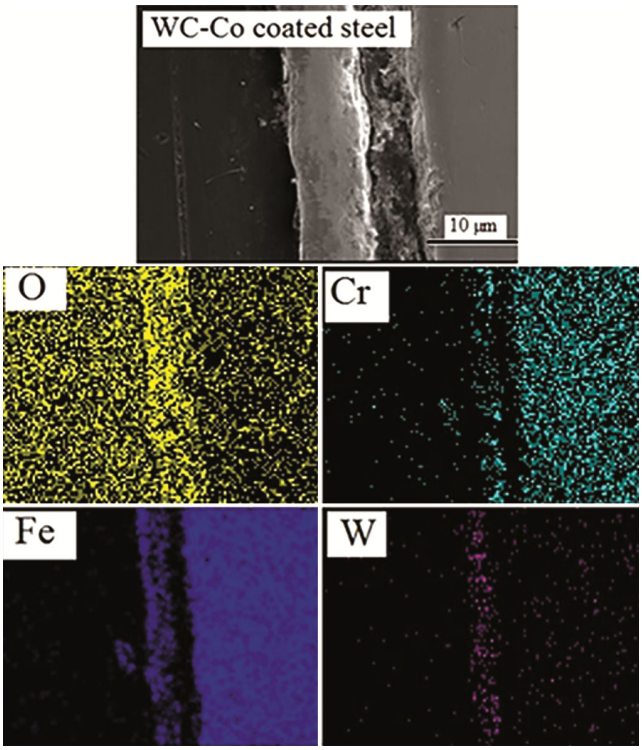


Fig. 14 — X-Ray mapping of WC-Co coated T91 steel after exposure in molten salt environment at 800 °C for 50 cycles in tubular furnace.

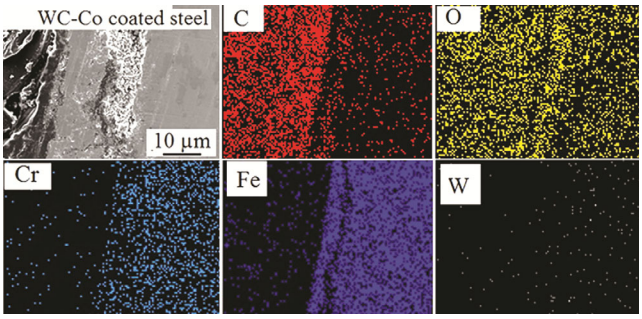


Fig. 15 — X-Ray mapping of WC-Co coated T91 steel after exposure in real bio-fuel fired boiler environment at 750±50 ºC for 48 hours.

occurred because of the coefficient of thermal expansion mismatch between the steel substrate and the coating composition. Although, the coating was intact before the experimentation, which depicts the good bond strength between the coating and the substrate provided by the detonation gun process as reported in the literature[11]. However, during hot corrosion experiments, the substrate and the coating experiences sudden thermal fluctuations. This creates the sudden contraction and expansion within the substrate and coating, thereby leading to delamination of the coating from the substrate. From weight gain graph (Fig. 4(a)) also, it can be depicted that WC-Co coated T91 steel suffered from very high weight gain starting from the 1st cycle till the 50th cycle. This might have occurred because of the formation of massive oxide on the substrate and base metal. Along with it, the delamination of coating also contributes to the weight gain. As after delamination the coating and the exposed substrate, both will form oxides. Whereas, both bare T91 steel and $Cr_3C_2$-NiCr coated T91 steel showed initial weight gain, which becomes constant after a few cycles. Initial weight gain occurred because of the formation of the oxides during exposure of the specimens at high temperature. However, the graph became constant after a few cycles, which shows that the oxide formed on the substrate was protective, which does not allow any diffusion from substrate towards the environment or vice versa. It was also seen from the graph that the weight gain of bare T91 steel was more as compared to $Cr_3C_2$-NiCr coated T91 steel. Such behavior of the graph shows the less protective nature of the substrate as compared to $Cr_3C_2$-NiCr coated T91 steel. Minor spallation also caused a higher weight gain of bare substrate. Graph shown in Fig. 4 (b) helps in identifying the parabolic behavior of substrates. From the parabolic rate constant, it can be predicted that $Cr_3C_2$-NiCr coated T91 steel shows the best resistance to corrosion under the given environment. Parabolic behavior of the graph also shows that the oxide formed on the substrate plays a protective role. Similar, results were observed in the actual environment as corrosion rate was maximum for WC-Co coated T91 steel and minimum for $Cr_3C_2$-NiCr coated steel.

SEM analysis for all three alloys was performed to observe the surface morphology and is shown in Figs (5-7) SEM analysis of $Cr_3C_2$-NiCr coated T91 steel (Fig. 6) shows the formation of dense needle-type oxide consisting of chromium and oxygen in major amount. Similar results of the formation of needle type oxide in case of $Cr_3C_2$-NiCr coating has been reported elsewhere[17].EDS analysis also indicates the presence of sodium and potassium, although the salt was applied only once before starting the experiments. The combination of the salts has eutectic temperature at 550ºC. Hence, the salts mixture will change its phase after reaching this temperature and thus it easily reacts with the protective oxide and forms other compounds. XRD analysis (Fig. 8) of the specimens also confirms the presence of compounds such as $K_2CrO_4$ in both bare and $Cr_3C_2$-NiCr coated

T91 steel. It was reported in the literature that $K_2CrO_4$ has a melting point higher than 1000ºC. As the test was conducted at 800ºC, potassium chromate was found in the oxide layer. It was also reported that formation of potassium chromate depletes the scale in chromia and it contributes to the formation of a non-protective, iron-rich scale in case of steel[18]. This might be one of the reasons that in bare T91 steel, minor chromium oxide peaks were formed although chromium was present in substantial amount in the substrate and chromium tend to form oxide when exposed at high temperature[19]. It was also found that, in the presence of a chlorine environment, the oxide combines with the chlorine to form volatile chlorides[4-6]. Due to presence of sulphur, iron forms FeS, which is a non-protective oxide. Sulfides generally form beneath the oxides causing more chromia spallation[20]. Hence, chromium was not seen in EDS analysis of bare T91 steel substrate. In X-ray mapping also (Figs 10 and 11), a very thin and light layer of chromium was seen at the substrate oxide interface. Oxide mainly consists of a thick layer of iron and oxygen. However, the reactions do not damage $Cr_3C_2$-NiCr coated steel as the coating remains intact to the steel and does not allow iron of base substrate to combine with the corrosive environment in a simulated environment. The coating will work as barrier between the environment and the base metal and provide protection by forming either $Cr_2O_3$ or $NiCr_2O_4$. This occurs as the coating will continuously supply chromium faster, thus providing protection. Presence of $Cr_2O_3$ was seen in XRD in case of $Cr_3C_2$-NiCr coated T91 steel when exposed in the simulated environment (Fig. 8) and $NiCr_2O_4$ when hanged in actual boiler environment (Fig. 9). Chromium oxide formed on the coating because of the conversion of chromium carbide to chromium oxide, as shown in reaction (Eq. 2)[21].

$$Cr_3C_2 \xrightarrow{+O_2} Cr_7C_3 \xrightarrow{+O_2} Cr_{23}C_6 \xrightarrow{+O_2} [Cr_{MET}] \xrightarrow{+O_2} Cr_2O_3 \quad \text{... (2)}$$

Although the oxide formed in the simulated environment seems dense and protective (Fig. 6(a), however, the oxide formed on the $Cr_3C_2$-NiCr coating (Fig. 6(b)) in the actual environment was porous. This indicates the aggressive nature of salt species produced due to burning of biofuel such as rice husk and wood in a boiler. EDS shows that actual atmosphere consists of calcium, silicon, along with sodium, potassium and sulfur. XRD (Fig. 9) also depicts the formation of oxides such as $Ni_2SiO_4$ and $CaCr_2O_4$ other than $K_2CrO_4$ and $NiCr_2O_4$. $Ni_2SiO_4$ formed by following reaction (Eq. 3):

$$2NiO + Sio_2 \rightarrow Ni_2SiO_4 \quad \text{... (3)}$$

Jacob *et al.*[22], in his study, reported the Gibbs free energy of nickel orthosilicate at different temperatures and confirmed its formation at 1000K due to more negative Gibbs free energy. Similarly, $CaCr_2O_4$ can be formed by the reaction of CaO and $Cr_2O_3$. Chiang *et al.*[23]mentioned in their study that CaO accelerates the degradation of $Cr_2O_3$ alloys by accelerating $CrO_3$ evaporation between 850ºC-1050ºC. A similar mechanism might be responsible for chromium oxide degradation in the present case, which eventually resulted in the porous oxide. This porous oxide will further allow the penetration of corrosive species inside the coating. X-ray mapping of $Cr_3C_2$-NiCr coated T91 steel (Fig. 13) after exposure in actual boiler environment indicates that iron was also present throughout the coating along with chromium, nickel and oxygen. This shows the diffusion of iron from substrate, whereas no such diffusion was observed in the case of a coated substrate (Fig. 12) exposed in a simulated environment which does not contain calcium.

Surface morphology of the oxide formed on WC-Co coated T91 steel (Fig. 7) indicated the formation of different type of oxide morphologies. Needle type, irregular shaped and rhombohedra shape oxide was formed mainly consisting of oxygen, tungsten, cobalt and iron. Kunioshi *et. al*[24], also conducted that an oxidation test on tungsten carbide-based coating at different temperatures and reported changes in morphology due to the presence of tungsten. EDS analysis shows the presence of a considerable amount of iron at some selected sites under both simulated and actual boiler environments. Iron might have present because of the exposure of the base metal due to the delamination of the coating. The presence of cobalt and tungsten indicates that although the coating was delaminated, the oxide of cobalt and tungsten was formed and remains there in the substrate. However, both were present in minor amount after the corrosion run in both simulated and actual environments. As already mentioned, the primary reason for this is the delamination of coating from the substrate. Also, tungsten carbide has a tendency to convert into $WO_3$

when exposed above 600ºC[25]. The conversion can be described by the following reactions given in Eqs (4 and 5).

$$WC + \frac{5}{2}O_2 \rightarrow WO_2 + CO_2 \quad \text{... (4)}$$

$$WC + 2O_2 \rightarrow WO_3 + CO \quad \text{... (5)}$$

However, the above reactions occurred while only oxygen or air is present. In the simulated environment, the specimens were exposed to a corrosive environment containing sulphur, potassium and chlorine. In the presence of these salts species, tungsten trioxide so formed further reacts with chlorine to form oxides such as $WO_2Cl_2$. The melting point of this compound is below 300ºC. This might be a reason that no peak of such compound was detected in XRD as the temperature is 800ºC in the test condition. Also, it was reported that $WO_3$ could evaporate due to its volatile nature[26]. X-ray mapping (Figs (14 and 15)) confirms that very thin layer of tungsten was left after corrosion run, thereby representing the unsuitability of WC-Co coating in the present environments.

## 4 Conclusion

The corrosion studies have been conducted in simulated and actual bio-fuel fired boiler environment. In simulated environment, compounds of sodium, potassium, chlorine and sulphur have been used. Whereas, in actual boiler environment, due to rice husk, compounds of silicon and calcium were also present.

- Formation of fragile and unprotective oxide was seen on the surface of bare T91 steel consisting of iron oxide and iron sulfides when exposed under simulated and actual boiler environment.
- $Cr_3C_2$-NiCr and WC-Co coatings have been successfully deposited on T91 steel using Detonation gun processes. But after exposure in simulated and actual boiler atmosphere, WC-Co coating got delaminated from the substrate after few cycles and $Cr_3C_2$-NiCr coating remains intact throughout the corrosion run.
- Although, $Cr_3C_2$-NiCr coating shows good corrosion resistance as compared to bare steel. However,chromia was attacked by both the atmospheres leading to porous oxide formation.
- Based on overall results, the corrosion resistance of the specimens studied in the present investigation has been found to be in the following order

WC-Co coated T91SS < T91SS < $Cr_3C_2$-NiCr coated T91 steel

## References


1 Rapp R A, *Corr Sci,* 44(2) (2002) 209.
2 Michelsen H P, Frandsen F, Dam-Johansen K, & Larsen O H, *Fuel Process Tech*, 54(1) (1998) 95.
3 Nielsen H P, Frandsen F J, Dam-Johansen K, & Baxter L L, *Prog Ener Comb Sci,* 26(3) (2000) 283.
4 Uusitalo M A, VuoristoP M J, & Mantyla T A, *Mater Sci & Eng A* 346(1-2) (2003) 168.
5 Zahs A, Spiegel M, & Grabke H, Mater and Corro, 50(10) (1999) 561.
6 Spiegel M, Zahs A, & Grabke H J, *Mater at High Temp,* 20(2) (2003) 153.
7 Chatha S S, Sidhu H S, & Sidhu B S, *Surf Coat Tech,* 206 (19) (2012) 3839.
8 Uusitalo M A, Vuoristo P M J, & Mantyla T A, *Corro Sci,* 46(6) (2004) 1311.
9 Murthy J K N, Rao D S, & Venkataraman B, *Wear,* 249(7) (2001) 592.
10 Saravanan P, Selvarajan V, Rao D S, Joshi S V, & Sundararajan G, *Surf Coat Tech,* 123(1)(2000) 44.
11 Singh L, Chawla V, & Grewal J S, *J Miner Mater Charac Eng*, 11(03) (2012) 243.
12 Zheng Z H O U, LuW A N G, Fu-Chi Wang, & Yan-Bo Liu, *Trans Nonferr Metal Soc,* 19 (2009) 634.
13 Chatha S S, Sidhu H S, & Sidhu B S, Adv Mater Res, 1137 (2016) 88.
14 Chatha S S, Sidhu H S, & Sidhu B S, *Surf Coat Tech*, 206(19-20) (2012) 4212.
15 Sidhu V P S, Goyal K, & Goyal R, J *Aust Ceram Soc*, 53(2) (2017) 925.
16 Parker G*, Encyc of Mater: Sci and Tech* (2001) 6285.
17 Mudgal D, Singh S, & Prakash S, *J Mat Eng Perf,* 24(1) (2015) 1.
18 Pettersson C, Pettersson J, Asteman H, Svensson J E, & Johansson L G, *CorroSci*, 48(6) (2006) 1368.
19 Kumar S, Mudgal D, Singh S, & Prakash S, *Adv Mater Lett*, 4(10) (2013) 754.
20 Sidhu T S, Agrawal R D, & Prakash S, *Surf Coat Tech,* 198 (1-3) (2005) 441.
21 Matthews S, James B, & Hyland M, *CorroSci,* 51(5) (2009) 1172.
22 Jacob K T, Kale G M, Ramachandran A K I L A, & Shukla A K, *High Temp Mat Pr*, 7(2-3) (1986) 141.
23 Chiang, K T, Meier, G H, & Perkins, R A, *J Mater Energy Systems,* 6(2)(1984) 71.
24 Kunioshi C T, Correa O V, & Ramanathan L V, *Surf Eng,* 22(2) (2006) 121.
25 Lofaj F, & Kaganovskii Y S, *J Mater Sci,* 30(7) (1995) 1811.
26 Babilius A, *Mater Sci,* 9(3) (2003) 183.